The RNA polymerase III repressor MAF1 is regulated by ubiquitin-dependent proteasome degradation and modulates cancer drug resistance and apoptosis

Received for publication, April 12, 2019, and in revised form, October 1, 2019 Published, Papers in Press, October 23, 2019, DOI 10.1074/jbc.RA119.008849

Xianlong Wang[‡], Aleksandra Rusin[‡], Christopher J. Walkey[‡], Justin J. Lin[§], and Deborah L. Johnson[‡1]

From the [‡]Department of Molecular and Cellular Biology, Baylor College of Medicine, Houston, Texas 77030 and [§]Zymo Research, Irvine, California 92614

Edited by George N. DeMartino

MAF1 homolog, negative regulator of RNA polymerase III (MAF1) is a key repressor of RNA polymerase (pol) III–dependent transcription and functions as a tumor suppressor. Its expression is frequently down-regulated in primary human hepatocellular carcinomas (HCCs). However, this reduction in MAF1 protein levels does not correlate with its transcript levels, indicating that MAF1 is regulated post-transcriptionally. Here, we demonstrate that MAF1 is a labile protein whose levels are regulated through the ubiquitin-dependent proteasome pathway. We found that MAF1 ubiquitination is enhanced upon mTOR complex 1 (TORC1)–mediated phosphorylation at Ser-75. Moreover, we observed that the E3 ubiquitin ligase cullin 2 (CUL2) critically regulates MAF1 ubiquitination and controls its stability and subsequent RNA pol III–dependent transcription. Analysis of the phenotypic consequences of modulating either CUL2 or MAF1 protein expression revealed changes in actin cytoskeleton reorganization and altered sensitivity to doxorubicin-induced apoptosis. Repression of RNA pol III–dependent transcription by chemical inhibition or knockdown of BRF1 RNA pol III transcription initiation factor subunit (BRF1) enhanced HCC cell sensitivity to doxorubicin, suggesting that MAF1 regulates doxorubicin resistance in HCC by controlling RNA pol III–dependent transcription. Together, our results identify the ubiquitin proteasome pathway and CUL2 as important regulators of MAF1 levels. They suggest that decreases in MAF1 protein underlie chemoresistance in HCC and perhaps other cancers and point to an important role for MAF1 and RNA pol III–mediated transcription in chemosensitivity and apoptosis.

RNA polymerase (pol)[2] III generates a variety of small noncoding RNAs. The majority of products include tRNAs and 5S rRNAs, which comprise essential components of the protein synthesis machinery. Rapid repression of RNA pol III–mediated transcription ensures cell survival during stress (1). MAF1 was originally identified in yeast as a repressor of this transcription process during diverse cellular environment stresses such as nutrient deprivation, rapamycin treatment, secretory defects, or DNA damage (2–4). Mechanically, MAF1 represses transcription initiation via its interaction with RNA pol III, which impairs recruitment of RNA pol III to the transcription initiation complex (5–7).

In mammals, MAF1 is also recruited to select RNA pol II–dependent gene promoters and act as a versatile transcription factor to either positively or negatively regulate gene expression. MAF1 represses the expression of the central transcription initiation factor TATA-binding protein (TBP) to regulate cell proliferation and oncogenic transformation (8). MAF1 also negatively regulates intracellular lipid accumulation by repressing transcription of the lipid biosynthesis genes FASN and ACC1 (9). Interestingly, MAF1 can also act as a transcription activator to enhance acetylation and activity of the PTEN promoter (10). Given that deregulation of MAF1-targeted genes are hallmarks of transformed cells and human cancers, it suggests MAF1 can function a tumor suppressor by regulating a subset of both RNA pol III– and pol II–dependent genes. Indeed, studies reveal that MAF1 inhibits cellular transformation and tumorigenesis (8, 10), and its expression is significantly down-regulated in primary human hepatocellular carcinomas (9, 10). Initial analysis revealed that this may also be observed in prostate cancers that are deficient for PTEN (9). Accumulating evidence supports the idea that enhanced RNA pol III–dependent transcription is necessary to drive oncogenesis (11, 12) and that alterations in the expression of specific tRNAs or tRNA derivatives are involved in proliferation, metastasis, and invasiveness of cancer cells, as well as tumor growth and angiogenesis in several malignant human tumors (13–17). These collective results indicate that the observed decrease in MAF1 protein expression and the resultant enhanced expression of MAF1 target genes provide an advantage to tumor cells beyond meeting the increased demand for overall protein synthesis.

This work was supported by NCI, National Institutes of Health Grants CA108614 and CA74138 (to D. L. J.). The authors declare that they have no conflicts of interest with the contents of this article. The content is solely the responsibility of the authors and does not necessarily represent the official views of the National Institutes of Health.

This article contains Tables S1–S3 and Figs. S1–S6.

[1] To whom correspondence should be addressed: Dept. of Molecular and Cellular Biology, Baylor College of Medicine, Houston, TX 77030. Tel.: 713-798-3560; Fax: 713-798-4032; E-mail: Deborah.Johnson@bcm.edu.

[2] The abbreviations used are: pol, polymerase; HA, hemagglutinin; $tRNA_i^{Met}$, initiator methionine tRNA; $tRNA^{Leu}$, leucine tRNA; HCC, human hepatocellular carcinoma; PTM, post-translational modification; LMB, leptomycin B; Ni–NTA, nickel–nitrilotriacetic acid; CRL, Cullin–RING ligase; HIF, hypoxia-inducible factor; vtRNA, vault RNA; MEF, murine embryonic fibroblast; GAPDH, glyceraldehyde-3-phosphate dehydrogenase; DAPI, 4,6-diamidino-2-phenylindole; sgRNA, single guide RNA; MTS, 3-(4,5-dimethylthiazol-2-yl)-5-(3-carboxymethoxyphenyl)-2-(4-sulfophenyl)-2H-tetrazolium.

MAF1 has been shown to be regulated by post-translational modifications (PTMs). Mammalian MAF1 is directly phosphorylated by mTORC1, primarily on serine 75, and this results in a 15% decrease in its ability to repress RNA pol III–dependent transcription (18–20). Mammalian MAF1 is predominantly nuclear, and it is retained in the nucleus upon phosphorylation by mTORC1 (18). Covalent SUMOylation on residue Lys-35 has been shown to impair MAF1 activity without changing MAF1 subcellular localization or expression (21), indicating that different residues and modifications can regulate MAF1 activity. Although these studies on the impact of PTMs of MAF1 and its influence on activity are compelling and informative, initial studies have revealed that significant decreases in MAF1 protein expression are observed in human HCC. Given that the PTMs so far identified do not appreciably alter MAF1 protein expression, we sought to understand how MAF1 expression is reduced in HCC and other cancer cells compared with normal epithelium.

Prior studies revealed that PTEN positively regulates cellular MAF1 protein amounts but not MAF1 mRNA (9), suggesting that the abundance of MAF1 protein is tightly controlled in cancer cells. This is consistent with the lack of observed changes in MAF1 transcripts in human cancers, despite the loss of MAF1 protein in tumors such as HCC. Here we reveal that MAF1 has a short half-life and that it is rapidly degraded through the ubiquitin/26S proteasome pathway. Ubiquitin/26S proteasome pathway–mediated regulation of MAF1 is dependent, at least in part, on mTORC1-mediated phosphorylation at serine 75. We also show that MAF1 is a substrate of the Cullin 2–based E3 ubiquitin ligase, which determines the MAF1 ubiquitination and its stability. Our results further reveal that alterations in cellular MAF1 protein expression and RNA pol III–dependent transcription affect chemoresistance and the ability of cells to undergo apoptosis.

Results

MAF1 is subjected to proteasome-mediated degradation

Previous studies showed MAF1 protein was significantly down-regulated in primary human HCC tumor samples relative to normal liver epithelium (9, 10). Interestingly, RNA-Seq analysis from the Gene Expression Profiling Interactive Analysis (GEPIA, http://gepia.cancer-pku.cn)[3] (22), based on the Cancer Genome Atlas (TCGA) and the Genotype-Tissue Expression (GTEx) data set for transcriptomic analysis, revealed that MAF1 transcript levels in liver tumor tissues tend to be higher compared with normal tissues (Fig. 1*A*). Given that there is little correlation between MAF1 mRNA expression with its protein expression, we considered that the substantial decrease in MAF1 protein previously observed in HCC relative to normal tissue might be a result of changes in protein stability. Therefore, MAF1 protein half-life was first measured in a variety of cell lines. A time course of cycloheximide treatment in human hepatocellular carcinoma (HepG2) and colorectal adenocarcinoma (HT-29) cell lines revealed that MAF1 protein is highly unstable with a half-life of less than 30 min (Fig. 1*B*), suggesting that MAF1 might be subject to post-transcriptional regulation. A similar result was also found in nontransformed human fibroblast MCF10A cell, arguing that the short half-life of MAF1 protein is not restricted to transformed cells (Fig. 1*B*). Because the major degradation pathway in eukaryotic cells is mediated through the proteasome system, we determined whether cells treated with proteasome inhibitors would accumulate MAF1 protein. Both HepG2 and HT29 cells displayed significant increases in MAF1 protein expression upon MG132 proteasome inhibitor treatment. MG132 treatment of A549 and H358 lung cancer cells showed similar results (Fig. S1*A*).

To better explore the mechanism contributing to the MAF1 protein stability, we engineered the HepG2 cell using CRISPR/Cas9 system to produce an endogenously expressed HA-tagged MAF1 protein (Fig. S1*B*). The resulting HepG2$^{MAF1-HA}$ cell line also exhibited substantial increases in MAF1 protein level (Fig. S1*C*) with no effect on MAF1 mRNA levels (Fig. 1*C*) upon inhibition of the proteasome by MG132 treatment. As expected, the accumulated MAF1 protein resulted in a decrease in expression of RNA pol III–dependent pre-tRNA$_i^{Met}$ and pre-tRNA^{Leu} transcripts (Fig. 1*C*). The rapid MAF1 turnover was significantly inhibited upon bortezomib treatment (Fig. 1*D*), confirming that MAF1 is subjected to proteasome-mediated degradation. In addition to proteasome-mediated degradation of MAF1, we further determined whether lysosomal-mediated degradation pathway might contribute to cellular steady-state levels of MAF1. Treatment of HepG2$^{MAF1-HA}$ cells with chloroquine to inhibit autophagy did not appreciably alter MAF1 protein expression (Fig. S1*D*). Together, these results reveal that MAF1 is rapidly turned over in cells via the proteasome pathway.

MAF1 degradation occurs in the nucleus in a ubiquitin-dependent manner

To determine whether the degradation of MAF1 occurs within the nucleus, we examined the effect of leptomycin B (LMB), a specific inhibitor of nuclear export, on MAF1 turnover. LMB inhibits the CRM-1–dependent nuclear export pathway through a covalent interaction at Cys-529 of CRM-1 (23) and has been used to determine whether nuclear export is required in the degradation of nuclear proteins. As shown in Fig. S2 (*A* and *B*), the turnover rate of MAF1 was comparable in the presence and absence of LMB. As a control, LMB blocked nuclear export of p53, resulting in an increase in its stability and nuclear accumulation, as reported previously (24). These results indicate that MAF1 is degraded in nuclear and preclude export as the mechanism for turnover of MAF1 proteins in the nucleus.

The ubiquitin–26S proteasome pathway is the main system for the intracellular protein degradation and turnover. During this process, the targeted protein is marked by covalent attachment of multiple ubiquitin molecules, which provide a recognition signal for the 26S proteasome (25). To investigate whether MAF1 is ubiquitinated, an HA-tagged MAF1 (MAF1–HA) construct was transiently expressed in 293T cells with or without a His-tagged ubiquitin construct. The cells were treated with or without MG132 and His-containing proteins were captured by nickel–nitrilotriacetic acid (Ni–NTA) beads

[3] Please note that the JBC is not responsible for the long-term archiving and maintenance of this site or any other third party hosted site.

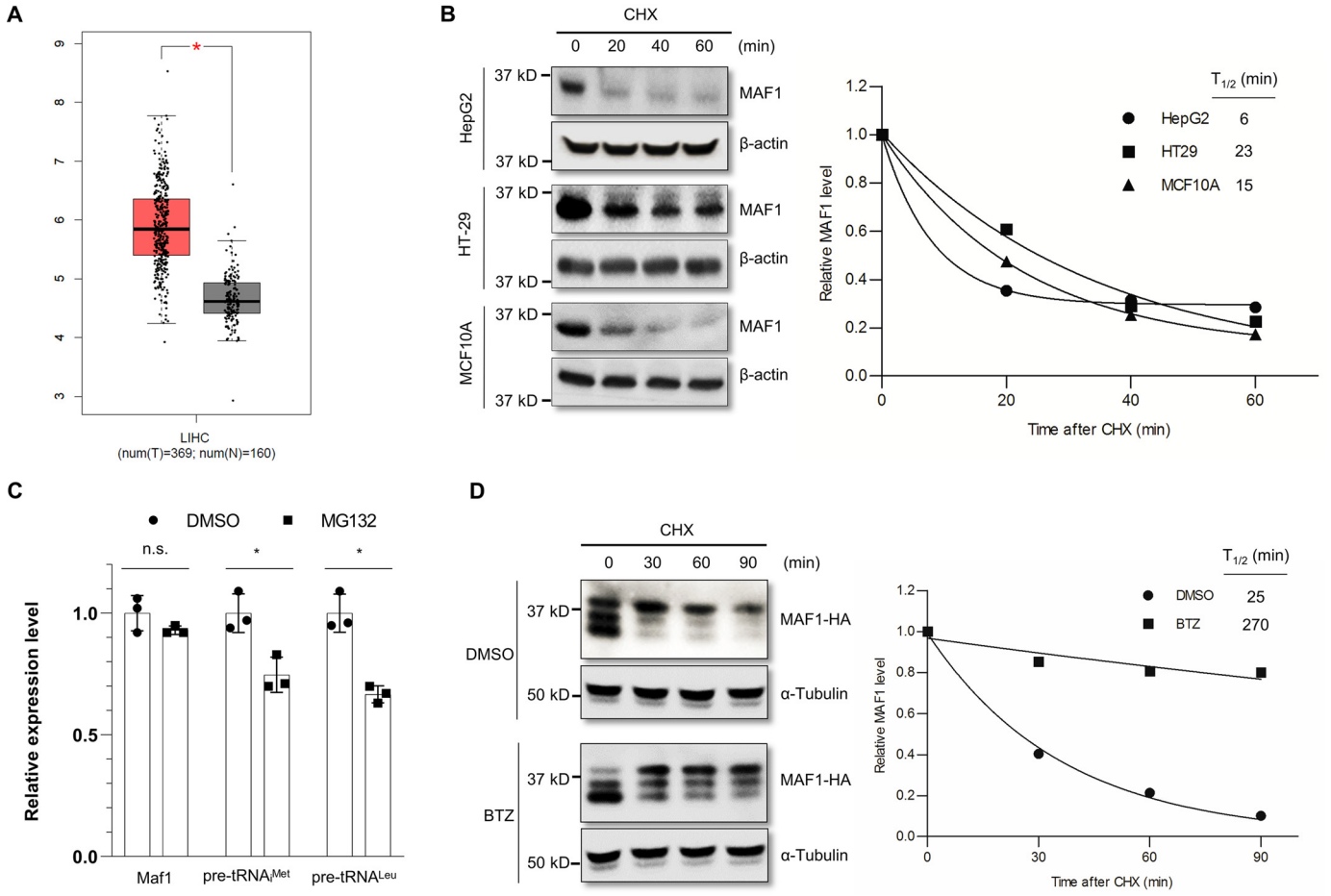

Figure 1. MAF1 is subjected to proteasome-mediated degradation. *A*, boxplot of the mRNA expression levels of MAF1 in liver hepatocellular carcinoma (*LIHC*) and normal control tissues. The images were taken from the GEPIA online database. The *red* and *black boxes* represent tumor and normal tissues, respectively. The data were obtained from the TCGA database. Tumor and control samples numbers are indicated. The *y* axis indicates the MAF1 gene expression levels. *, $p < 0.05$. *B*, *left panel*, HepG2, HT-29, and MCF10A cells were incubated with 100 μg/ml cycloheximide (*CHX*) for the indicated time intervals. The cell lysates were then prepared and analyzed by immunoblotting using MAF1 and β-actin antibodies. *Right panel*, densitometric quantification of MAF1 protein levels (normalized to β-actin). The half-life values were calculated by one-phase decay curve fitting using GraphPad Prism software and are denoted as $T_{1/2}$. *C*, HepG2$^{MAF1-HA}$ cells were treated with vehicle (DMSO) or MG132 (10 μM) for 4 h. Total RNA was isolated, and qRT-PCR analysis was performed with primers specific for MAF1 and precursor $tRNA_i^{Met}$ and $tRNA^{Leu}$. The amount of transcript was normalized to GAPDH. The values shown are the means ± S.E. (n = 3). The fold change was calculated relative to the amount of transcript expressed in vehicle group. *, $p < 0.05$, Student's *t* test. *D*, *left panel*, HepG2-HA cells were treated with vehicle or bortezomib (*BTZ*) (500 nM) for 4 h, and then cells were treated with 100 μg/ml CHX and harvested at the indicated time periods. Cell lysates were then prepared and analyzed by immunoblotting using HA and α-tubulin antibodies. *Right panel*, densitometric quantification of MAF1–HA protein levels (normalized to α-tubulin). The half-life values are denoted as $T_{1/2}$.

under denaturing conditions. The ubiquitinated MAF1 species were detected by immunoblot analysis with anti-HA antibody. Higher molecular weight polyubiquitinated species were detected only when His– ubiquitin was expressed (Fig. 2*A*). These bands were more pronounced when cells were treated with MG132. Similar results were observed in HT-29 cells where MG132 enhanced the endogenous ubiquitination of ectopically expressed MAF1 (Fig. S2*C*). These results demonstrate that MAF1 is polyubiquitinated.

Ubiquitin conjugation of proteins may involve seven distinct ubiquitin lysine residues (Lys-6, Lys-11, Lys-27, Lys-29, Lys-33, Lys-48, and Lys-63) (26). Lys-48 –linked chains are the predominant linkage type and mainly used for targeting modified substrates for the 26S proteasome–mediated degradation (26). Using a linkage-specific antibody that recognizes polyubiquitin chains joined through Lys-48, we observed that Lys-48 linkage–specific ubiquitination chains are present on MAF1 (Fig. S2*D*). To further confirm that the ubiquitin–26S proteasome pathway is involved in MAF1 degradation, we blocked the activity of the 26S proteasome in HepG2$^{MAF1-HA}$ cells by knockdown of PSMD1, a key component of 19S regulator lid that recognizes the polyubiquitinated substrate and channels the substrate into the catalytic 20S core of the proteasome. Knockdown of PSMD1 has been shown to be an approach to inhibit the 26S proteasome activity by inhibiting 19S function. This was shown to produce accumulation of p53 protein by inhibiting its degradation (27). Similar to p53, decreased PSMD1 expression increased MAF1 protein level and extended its half-life (Fig. 2*B*). These data indicate that MAF1 degradation requires the presence of a functional intact 26S proteasome complex.

In addition to the 19S lid, the proteasome activator REGγ can form an 11S regulatory cap to activate the 20S proteasome (28). Recent studies showed that REGγ can target intact proteins, such as SRC-3 and p21, for degradation in a ubiquitin- and ATP-independent manner (29–31). To explore whether REGγ is required for MAF1 degradation, its expression was inhibited.

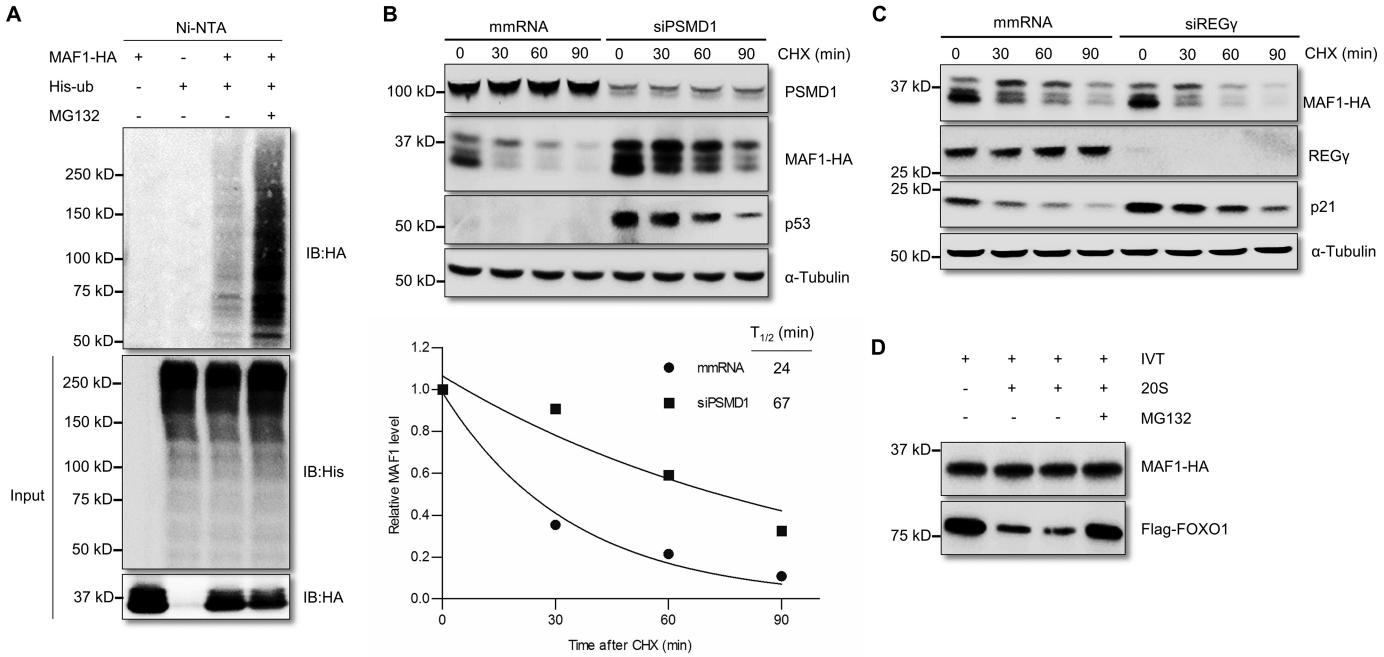

Figure 2. MAF1 degradation is ubiquitin-dependent. *A*, MAF1 is ubiquitinated *in vivo*. 293T cells were cotransfected with plasmids expressing His-tagged ubiquitin and HA-tagged MAF1 as indicated for 36 h. The cells were treated with vehicle or MG132 (10 μM) for 6 h before harvest. Ubiquitinated proteins were pulled down using Ni–NTA–agarose, and these and whole-cell lysates were analyzed by immunoblotting (*IB*) with the indicated antibodies. *B*, *upper panel*, HepG2$^{MAF1-HA}$ cells were transiently transfected with nonsilencing scrambled mismatch RNA (*mmRNA*) or siRNA targeting PSMD1 for 48 h, and then cells were treated with 100 μg/ml CHX and harvested at the indicated time periods. Cell lysates were then prepared and analyzed by immunoblotting using PSMD1, HA, p53, and α-tubulin antibodies. *Lower panel*, densitometric quantification of MAF1 protein levels (normalized to α-tubulin). The half-life values are denoted as $T_{1/2}$. *C*, HepG2$^{MAF1-HA}$ cells were transiently transfected with scrambled mismatch RNA or siRNA targeting REGγ for 48 h, and then cells were treated with 100 μg/ml CHX and harvested at the indicated time periods. The cell lysates were then prepared and analyzed by immunoblotting using HA, REGγ, p21, and α-tubulin antibodies. *D*, indicated *in vitro* transcribed and translated (*IVT*) proteins (HA-tagged MAF1 or FLAG-tagged Foxo1) were incubated with or without purified human proteasome 20S for 2 h. MG-132 (10 μM) was added where indicated to inhibit proteasome activity in the reaction. The MAF1 and FOXO1 protein degradation was analyzed by immunoblotting using HA and FLAG antibodies, respectively. *CHX*, cycloheximide.

Although decreased REGγ expression increased the steady-state level of p21 protein, no effect on MAF1 expression or its turnover rate was observed (Fig. 2*C*). As has been reported for a growing number of proteins (32–34), the core 20S proteasome itself has been shown to degrade proteins in a ubiquitin-independent manner. To test this, *in vitro* translated proteins were incubated with the 20S proteasome complex. FOXO1 protein, which has been shown to be degraded *in vitro* by the 20S proteasome (35), was used as a positive control. Similar with previously published reports, FOXO1 was efficiently degraded by purified 20S proteasomes. Under these conditions, however, MAF1 protein remained stable (Fig. 2*D*). Thus, neither the REGγ nor the 20S proteasome are capable of regulating MAF1 turnover either *in vivo* or *in vitro*. These results indicate that MAF1 degradation is mediated in a ubiquitin-dependent 26S proteasome manner.

Phosphorylation of MAF1 on Ser-75 affects its ubiquitination and stability

Previous studies have shown that phosphorylation of proteins may regulate ubiquitination and the subsequent degradation of proteins (36). Because mTORC1 phosphorylates MAF1, primarily at Ser-75, resulting in a decrease in its ability to repress transcription, we determined whether Ser-75 phosphorylation affects MAF1 degradation. In agreement with previous studies (19), treatment with the mTORC1 inhibitor, rapamycin, resulted in enhanced dephosphorylation of MAF1 (*lower band shift*, Fig. 3*A*). A moderate increase in total MAF1 protein level was also observed together with an extended half-life (Fig. 3*A*). This was a direct result of mTORC1-mediated phosphorylation because the phospho-resistant MAF1 S75A also similarly extended the half-life of MAF1 protein (Fig. 3*B*). MAF1 is also phosphorylated by mTOR on Ser-60 and Ser-68 (19). However, S60A/S68A/S75A triple mutation did not further extend MAF1 half-life beyond that of the Ser-75 single mutation (Fig. S3*A*), indicating that Ser-75 phosphorylation status plays a critical role in mTORC1 regulation of MAF1 turnover. Furthermore, MAF1 S75A had a marked reduction in ubiquitination, whereas the phosphomimic S75D (serine to aspartic acid) mutant displayed enhanced ubiquitination compared with WT MAF1 (Fig. 3*C*). Collectively, our results suggest that mTORC1-mediated phosphorylation is involved in MAF1 ubiquitination and turnover. Notably, mTOR kinase inhibition only delays MAF1 turnover. To confirm this observation, the cells were treated with MG132 alone or in the presence of rapamycin. MG132 accumulated MAF1 protein along with inhibiting mTORC1 activity. However, it failed to abolish the phosphorylation states of MAF1. Importantly, MAF1 expression was still sensitive to MG132 treatment (Fig. S3*B*), suggesting the existence of additional regulatory mechanisms for its degradation.

Cullin 2 RING E3 ligase ubiquitinates MAF1 to target it for proteasomal degradation

Cullin–RING ligases (CRLs), the largest of the E3 ubiquitin ligase family, promotes ubiquitination and degradation of var-

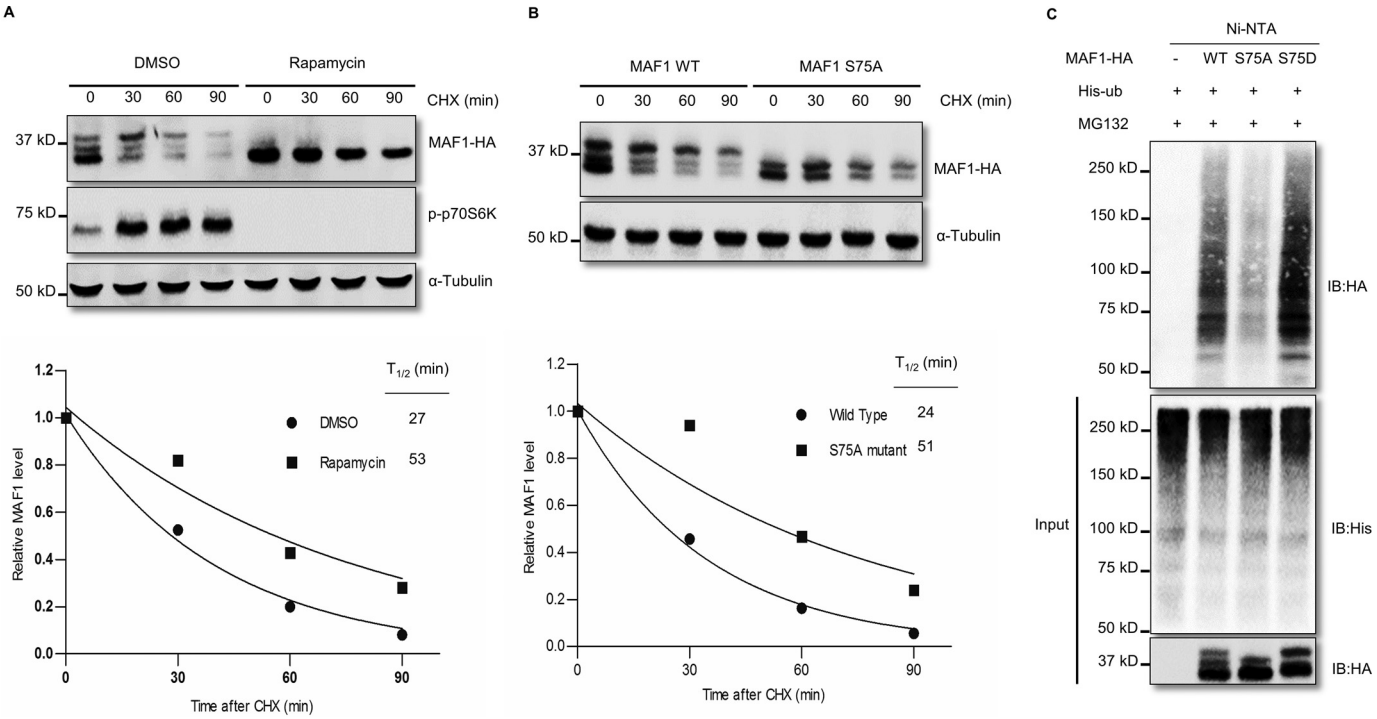

Figure 3. Phosphorylation of MAF1 on Ser-75 affects its ubiquitination and stability. *A*, *upper panel*, HepG2$^{MAF1-HA}$ cells were treated with vehicle or rapamycin (20 nM) for 6 h, and then cells were treated with 100 μg/ml cycloheximide (*CHX*) and harvested at the indicated time periods. Cell lysates were then prepared and analyzed by immunoblotting (*IB*) using HA, phospho-p70 S6 kinase (Thr-389), and α-tubulin antibodies. *Lower panel*, densitometric quantification of MAF1 protein levels (normalized to α-tubulin). The half-life values are denoted as $T_{1/2}$. *B*, *upper panel*, HepG2 cells were transfected with plasmids expressing HA-tagged WT or S75A mutant MAF1 as indicated for 36 h, and then cells were treated with 100 μg/ml CHX and harvested at the indicated time periods. The cell lysates were then prepared and analyzed by immunoblotting using HA and α-tubulin antibodies. *Lower panel*, densitometric quantification of MAF1 protein levels (normalized to α-tubulin). The half-life values are denoted as $T_{1/2}$. *C*, 293T cells were cotransfected with plasmids expressing His-tagged ubiquitin, HA-tagged WT, or S75A or S75D mutant MAF1 as indicated for 36 h. The cells were treated with MG132 (10 μM) for 6 h before harvest. Ubiquitinated proteins were pulled down using Ni–NTA–agarose, and these and whole-cell lysates were analyzed by immunoblotting with the indicated antibodies.

ious cellular key regulators involved in a broad array of physiological and pathological processes (37). MLN4924 selectively inhibits CRLs activity by blocking the conjugation of NEDD8 to the Cullin protein (38). As shown in Fig. S4*A*, MLN4924 treatment caused a marked accumulation of MAF1 protein, suggesting that CRLs were involved in MAF1 regulation. To further identify the Cullin proteins that mediate MAF1 degradation, we knocked down the expression of the individual CUL1, 2, 3, and 4A proteins. Decreased expression of only CUL2, and not the other Cullins, caused a significant accumulation of MAF1 protein (Fig. 4*A* and Fig. S4*B*) without changing MAF1 mRNA expression and produced subsequent decreases RNA pol III–dependent pre-tRNA$_i^{Met}$ and pre-tRNA^{Leu} transcripts (Fig. 4*B*). In addition, decreased CUL2 expression resulted in a slight decrease in MAF1 ubiquitination (Fig. 4*C*) and a significant extension of its half-life (Fig. 4*D*). Together, these results identify MAF1 as a CUL2 substrate and a mechanism by which cellular MAF1 protein amount is regulated.

We further tested a potential role for the von Hippel–Lindau tumor suppressor protein (VHL), a specific adaptor protein for CUL2, in the recruitment of MAF1 to the CUL2 ligase complex. VHL participates in the degradation of hypoxia-inducible factor-1α (HIF1α) mediated by CUL2 ligases (39). Previous results showed that RNA Pol III transcription is suppressed upon hypoxic stress (40). In agreement with previous studies, our results also confirmed that CUL2 knockdown resulted in the accumulation of HIF1α protein (Fig. 4*A*). However, unlike the HIF1α protein, hypoxic stress greatly down-regulated MAF1 protein expression (Fig. S4*C*). Moreover, VHL knockdown did not affect MAF1 protein levels (Fig. S4*D*). These results suggest that MAF1 is degraded in a CUL2-dependent way that does not involve VHL.

MAF1 regulates CUL2-mediated actin cytoskeleton remodeling and doxorubicin resistance

We next sought to determine the phenotypic consequences of CUL2-mediated modulation of MAF1 expression. We first analyzed whether alterations in CUL2 would promote changes in the cell cycle. Consistent with previous studies (41), no changes in the distribution of cells within the cell cycle were observed (Fig. S5, *A* and *B*). Previous work reported that changes in CUL2 expression are associated with actin cytoskeleton reorganization and cell motility (41). Our previous work also revealed striking morphological changes and enhanced stress fiber formation that accompanied decreases in MAF1 expression (8). Therefore, we considered the possibility that CUL2 regulates actin cytoskeleton remodeling through its ability to manipulate MAF1 protein levels. As expected, cells with reduced CUL2 expression exhibited remarkable decrease in the abundance of stress fiber formation, whereas MAF1 knockdown cells showed increased

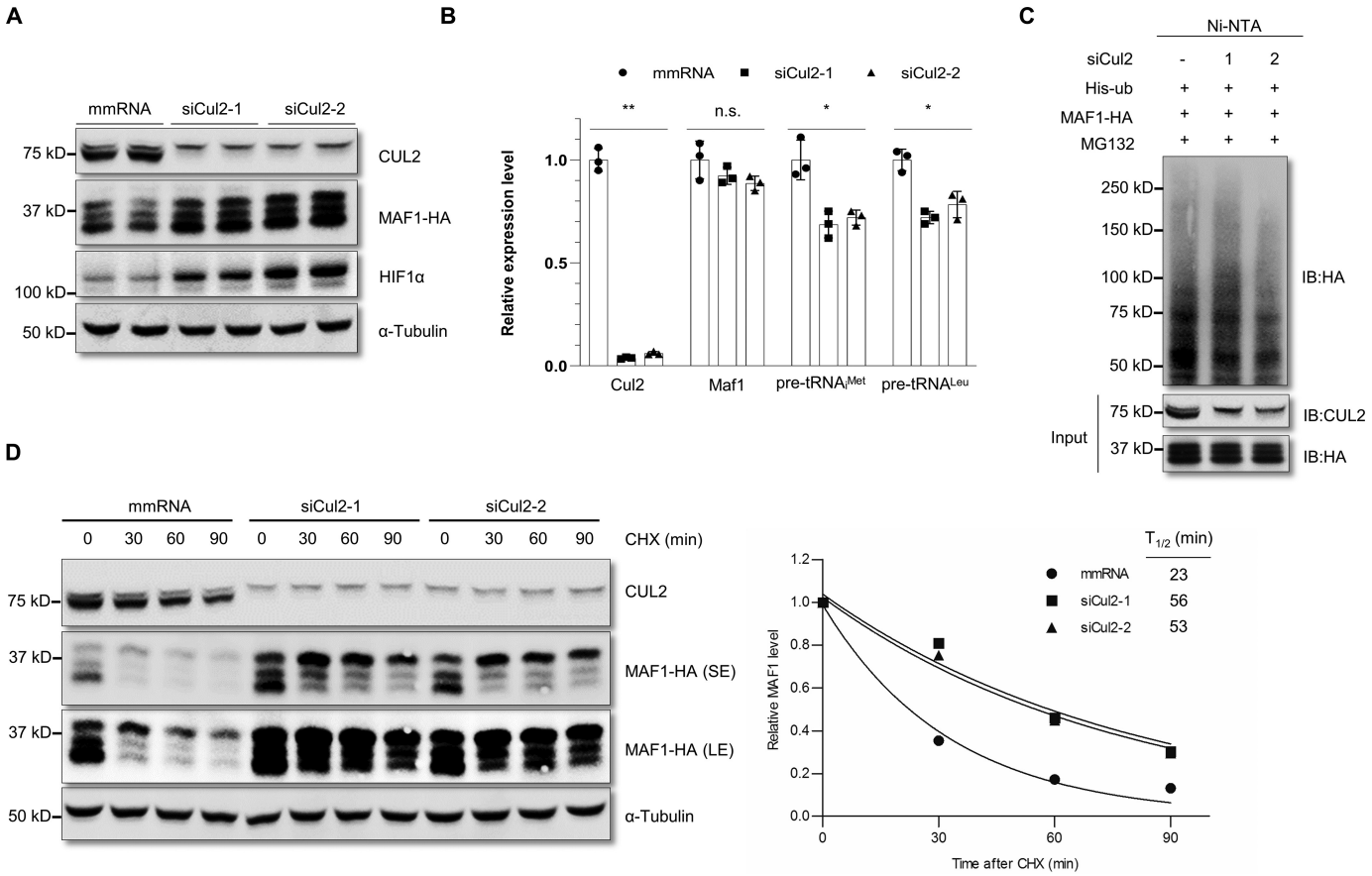

Figure 4. Cullin 2 RING E3 ligase ubiquitinates MAF1 to target it for proteasomal degradation. *A*, HepG2$^{MAF1-HA}$ cells were transiently transfected with scrambled mismatch RNA (*mmRNA*) or siRNA targeting Cul2 for 48 h. The cell lysates were then prepared and analyzed by immunoblotting (*IB*) using CUL2, HA, HIF1α, and α-tubulin antibodies. *B*, HepG2$^{MAF1-HA}$ cells were transiently transfected with scrambled mismatch RNA or siRNA targeting Cul2 for 48 h. Total RNA was isolated, and qRT-PCR analysis was performed with primers specific for Cul2, Maf1, and precursor $tRNA_i^{Met}$ and $tRNA^{Leu}$. The amount of transcript was normalized to GAPDH. The values shown are the means ± S.E. (n = 3). The fold change was calculated relative to the amount of transcripts expressed in vehicle group. **, $p < 0.01$; *, $p < 0.05$, Student's *t* test. *C*, 293T cells were transiently transfected with scrambled mismatch RNA or siRNA targeting Cul2 for 24 h, and then cells were cotransfected with plasmids expressing HA-tagged MAF1 and His-tagged ubiquitin as indicated for another 24 h. The cells were treated with MG132 (10 μM) for 6 h before harvest. Ubiquitinated proteins were pulled down using Ni–NTA–agarose, and these and whole-cell lysates were analyzed by immunoblotting with the indicated antibodies. *D*, *left panel*, HepG2$^{MAF1-HA}$ cells were transiently transfected with scrambled mismatch RNA or siRNA targeting Cul2 for 48 h, and then cells were treated with 100 μg/ml cycloheximide (*CHX*) and harvested at the indicated time periods. The cell lysates were then prepared and analyzed by immunoblotting using CUL2, HA, and α-tubulin antibodies. *Right panel*, densitometric quantification of MAF1–HA protein levels (normalized to α-tubulin). The half-life values are denoted as $T_{1/2}$.

stress fiber indicated by phalloidin staining (Fig. 5*A*). Importantly, double knockdown of CUL2 and MAF1 suppressed the CUL2 knockdown phenotypes. Stress fiber abundance was partially restored in the cells treated with both CUL2 siRNA and MAF1 siRNA, to an extent comparable with control cells (Fig. 5*A*). Thus, our data support the model that MAF1 acts as an important regulator in CUL2-mediated actin stress fiber integrity.

Targeting the actin cytoskeleton of cancer cells to reduce tolerance to chemotherapy offers a valuable strategy in cancer treatment (42). We therefore investigated whether CUL2 or/and MAF1 knockdown altered the sensitivity of cells to doxorubicin, a chemotherapeutic agent commonly used in metastatic hepatocellular carcinoma and other cancer treatments (43). Upon doxorubicin treatment, the relative viability cell population of CUL2 knockdown cell was markedly decreased compared with control cells measured by MTS assays (Fig. 5*B*), suggesting that CUL2 knockdown enhanced the sensitivity of cells to doxorubicin treatment. Interestingly, reduced MAF1 expression resulted in a moderately increased proportion of live cells than the control group treated with low doses of doxorubicin (Fig. 5*B*), indicating that decreased MAF1 expression protects against doxorubicin-induced cell death. Moreover, reduction in both CUL2 and MAF1 had similar sensitivities to doxorubicin as control cells, suggesting that decreases in MAF1 could restore doxorubicin resistance in cells with reduced expression of CUL2 (Fig. 5*B*).

Because apoptosis is the major type of cell death triggered by chemotherapy drugs, we further evaluated whether the observed changes in sensitivity to doxorubicin were associated with apoptosis. Apoptosis was evaluated by flow cytometry with annexin V–FITC and propidium iodide labeling and immunoblotting for cleaved caspase-3. In untreated cells, decreased expression of CUL2, MAF1, or both proteins simultaneously did not reveal significant changes in apoptosis (Fig. S5*C*). However, cells with transient decreases in CUL2 were more susceptible to undergo apoptosis upon doxorubicin treatment. In contrast, MAF1 knockdown led to a significant decrease in the fraction of apoptotic cells. Furthermore, MAF1 decreases attenuated the observed increases in doxorubicin-

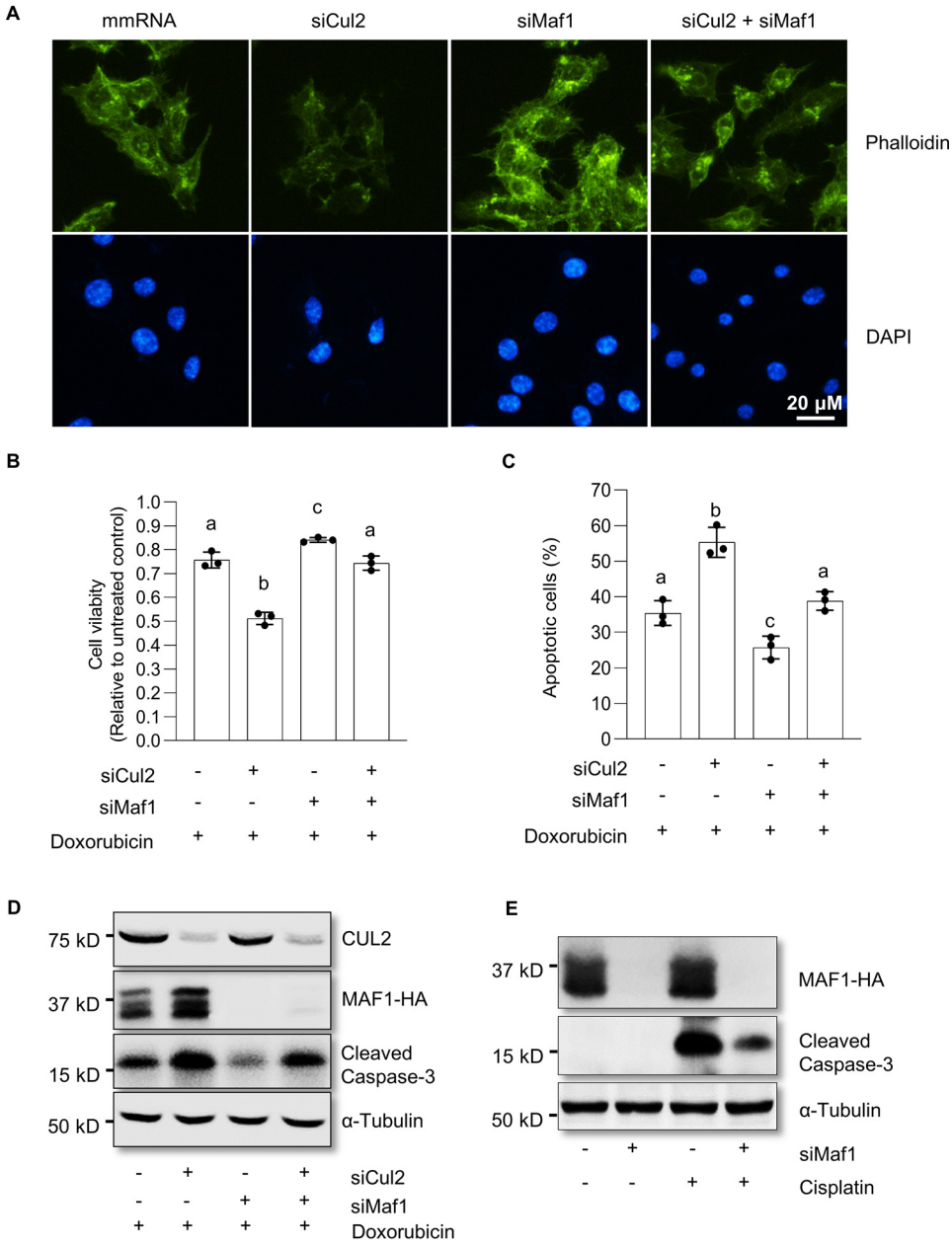

Figure 5. MAF1 regulates CUL2-mediated actin cytoskeleton remodeling and doxorubicin resistance. *A*, HepG2$^{MAF1-HA}$ cells were transiently transfected with scrambled mismatch RNA (*mmRNA*), siRNA targeting Cul2, Maf1, or a mix of siRNA (Cul2 and Maf1) for 48 h. The cells were fixed and stained for F-actin (*green*, phalloidin-FITC) and cell nuclei (*blue*, DAPI). Original magnification, 40×. *B*, HepG2$^{MAF1-HA}$ cells were transiently transfected with siRNAs as indicated for 48 h, and then the cells were treated with 0.5 μM doxorubicin for another 24 h. Cell viability was assessed by MTS assay. *C*, apoptosis was measured by flow cytometry analysis after the cells were double-stained with annexin V and propidium iodide. The data from the bar graphs represent the means ± S.D. of apoptosis (%) from three independent experiments. $^{a-d}$, means without a common superscript differed ($p < 0.05$). *D*, cell lysates were then prepared and analyzed by immunoblotting using CUL2, HA, cleaved caspase-3, and α-tubulin antibodies. *E*, HepG2$^{MAF1-HA}$ cells were transiently transfected with siRNAs as indicated for 48 h, and then the cells were treated with 25 μM cisplatin for another 24 h. The cell lysates were then prepared and analyzed by immunoblotting using HA, cleaved caspase-3, and α-tubulin antibodies.

induced apoptosis mediated by decreased CUL2 expression (Fig. 5*C* and Fig S5*C*). These changes in apoptosis were confirmed by examining changes in cleaved caspase-3 from a parallel experiment (Fig. 5*D*). In addition, our results also show MAF1 knockdown has similar protective effects on the cleavage of caspase 3 induced by cisplatin (Fig. 5*E*), another chemotherapy drug used to treat various human cancers. It suggests that MAF1 plays a critical common role in regulating apoptosis and chemoresistance.

Repression of RNA pol III–mediated transcription results in enhanced doxorubicin sensitivity

Given the role of MAF1 in repressing RNA polymerase III–dependent transcription, we hypothesized that the observed function of MAF1 in drug resistance was attributed to its ability to repress RNA polymerase III–mediated transcription. To test this, we first used an RNA pol III–specific chemical inhibitor, ML-60218 (44). ML-60218 inhibitor treatment promoted doxorubicin-induced cell death and cleaved caspase-3 expres-

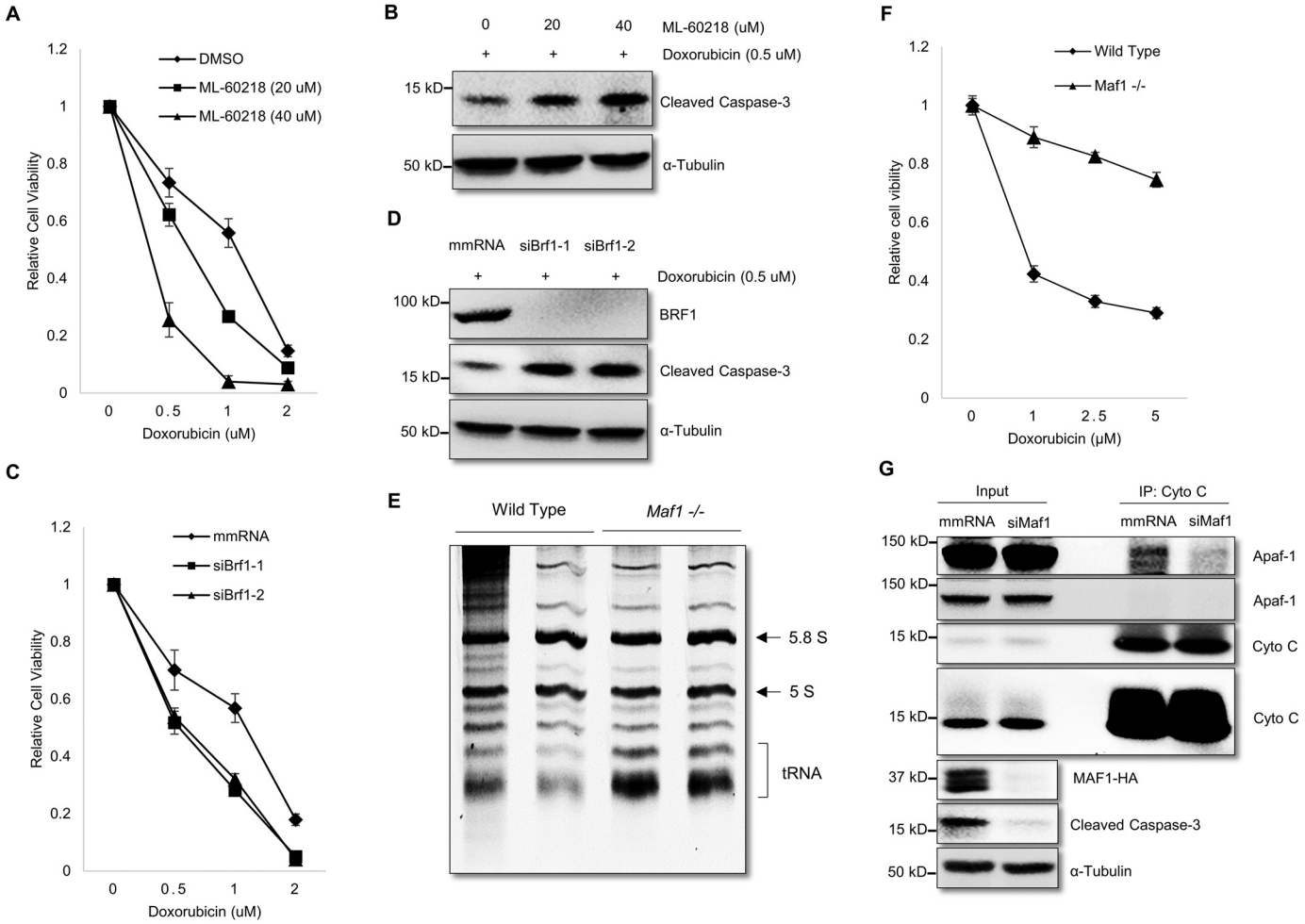

Figure 6. RNA pol III repression results in enhanced doxorubicin sensitivity. *A*, dose-dependent cell growth inhibition curves of HepG2$^{MAF1-HA}$ cells (pretreated with 20 or 40 μM ML-60218 for 16 h) treated with different concentrations of doxorubicin for 24 h. *C*, dose-dependent cell growth inhibition curves of HepG2$^{MAF1-HA}$ cells (transfected with siRNAs as indicated for 48 h) treated with different concentrations of doxorubicin for 24 h. Cell viability was assessed by MTS assay. Each *dot* and *error bar* on the *curves* represents the mean ± S.D. *B* and *D*, HepG2$^{MAF1-HA}$ cells were treated as *A* and *C*. Cell lysates were then prepared and analyzed by immunoblotting using cleaved caspase-3, BRF1, and α-tubulin antibodies. *E*, total RNAs from the WT MEFs or *Maf1*$^{-/-}$ MEFs were resolved on 8% urea-containing PAGE and visualized by gel red. 5.8S rRNA, 5S RNA, and tRNA are indicated by *arrows* or *brackets*. *F*, WT MEFs and *Maf1*$^{-/-}$ MEFs were exposed to different concentration of doxorubicin for 24 h, and then cell viability was measured by MTS cell proliferation assay. Each *dot* and *error bar* on the curves represents the mean ± S.D. *G*, HepG2$^{MAF1-HA}$ cells were transiently transfected with scrambled mismatch RNA (*mmRNA*) or siRNA targeting Maf1 for 48 h, and then cells were treated with 0.5 μM doxorubicin for another 24 h. The cell lysates were then prepared and subjected to immunoprecipitation (*IP*) with anti–cytochrome (*Cyto*) *c*. The resulting immune complexes, as well as whole-cell lysates, were analyzed by immunoblotting with the indicated antibodies.

sion in a dose-dependent manner (Fig. 6, *A* and *B*). To verify these results, a second approach was used to repress RNA pol III–dependent transcription. Down-regulation of BRF1, an RNA pol III–specific TFIIIB transcription factor subunit (45), also produced a decrease in cell viability and an increase in cleaved caspase-3 expression in the presence of doxorubicin (Fig. 6, *C* and *D*). We also confirmed our results using MAF1-deficient (*Maf1*$^{-/-}$) mouse embryonic fibroblast cells (MEFs). Compared with WT MEFs, *Maf1*$^{-/-}$ MEFs exhibited higher level of mature tRNAs abundance (Fig. 6*E*) and showed much more resistance to doxorubicin-induced cell death (Fig. 6*F*). Reconstitution of *Maf1*$^{-/-}$ MEFs with ectopic expression of the constitutively active mutant MAF1 S75A (Fig. S6*A*) decreased the RNA pol III–dependent pre-tRNA^{Ile} and pre-tRNA^{Leu} transcripts (Fig. S6*B*) and enhanced doxorubicin sensitivity (Fig. S6*C*). These results indicate that MAF1-mediated regulation of drug resistance can be recapitulated by repressing RNA pol III–dependent transcription.

Recent evidence has shown that dysregulation in the expression and function of tRNAs and tRNA derivatives play important roles in cancer progression (13–17). Both mature tRNAs and tRNA halves were reported to bind to cytochrome *c* and impair the association of cytochrome *c* with Apaf-1, which then blocks the formation of the apoptosome and the subsequent activation of caspases (46, 47). To further determine whether the observed changes in drug resistance by RNA pol III–mediated transcription might be specifically mediated through changes in tRNAs, we examined whether the association of cytochrome *c* with Apaf-1 was impaired when RNA pol III–dependent transcription was induced by decreases in MAF1 expression. Interestingly, the expression of both cytochrome *c* and Apaf-1 basal levels were not altered upon reduced MAF1

expression (Fig. 6*G*). However, the amount of Apaf-1 that was associated with cytochrome *c* was drastically decreased upon MAF1 knockdown (Fig. 6*G*). These results indicate that decreases in MAF1 expression and concomitant increases in tRNA expression inhibit the formation of cytochrome *c*–Apaf-1 complexes, thereby blocking apoptosis. Our collective results support the idea that at least one mechanism by which MAF1 functions to promote drug resistance and inhibit apoptosis is through its ability to repress RNA pol III–dependent tRNA gene transcription.

Discussion

Given the important functions of MAF1 in controlling lipid metabolism and oncogenesis, a better understanding of the mechanisms by which MAF1 is regulated and dysregulated in cancer will facilitate the development of new cancer therapeutic strategies. MAF1 serves as a central repressor for RNA pol III–dependent transcription. Induction of RNA pol III–mediated transcription is a hallmark of human cancers, and evidence supports that this is necessary for oncogenic transformation (11). MAF1 functions as a tumor suppressor, and its expression has been shown to be substantially decreased in HCC (9, 10), contributing to the overall enhancement of RNA pol III–mediated transcription. We find that MAF1 is a labile protein with a short half-life in multiple different cell lines. Our results demonstrate that ubiquitin-dependent proteasome-mediated degradation is a key mechanism by which MAF1 protein expression is regulated. Bortezomib is a proteasome inhibitor that has shown impressive efficacy in the treatment of multiple human cancers (48). Previous studies showed that the anti-cancer activity of bortezomib is associated with its ability to down-regulate various RNA pol II–dependent anti-apoptotic genes (49). Our results have discovered a previously unknown function for bortezomib that contributes to its therapeutic effects. Enhancing the stability of MAF1 and its subsequent repression of RNA pol III–dependent transcription may also augment its ability to promote apoptosis and facilitate tumor cell death.

Ubiquitination is a very common post-translational covalent modification that plays a role in diverse physiological functions, including transcription. Numerous studies indicate that ubiquitination plays critical role in regulating RNA pol II–dependent transcription (50–52), whereas the potential role of ubiquitination on RNA pol I– or pol III–dependent gene expression remains poorly understood. Recently, the largest catalytic RNA pol III subunit in yeast, C160, was found to be ubiquitinated and degraded by the proteasome upon stress (53). Alterations in C160 degradation controls RNA pol III activity and its association with chromatin (54). In our current study, we have identified a key molecular event by which ubiquitination exerts a positive effect on RNA pol III–dependent transcription by promoting MAF1 degradation in human cells. Although ubiquitination most often leads to proteasome-mediated degradation of the target protein, recent evidence suggests nonproteolytic functions for ubiquitination in the regulation of protein subcellular localization and activity. Wang *et al.* (55) reported that a RING domain–containing ubiquitin E3 ligase RNF12 catalyzed Lys-27– and Lys-33–linked ubiquitination of the RNA pol III–specific TFIIIB subunit, BRF1. Independent of BRF1 degradation, this modification negatively regulates RNA pol III–dependent transcription by impeding the binding of BRF1 to target gene promoters (55). These results suggest that ubiquitination can play distinct roles in the regulation of RNA pol III–dependent transcription, depending on the protein that is targeted and which type of polyubiquitin chains are formed within the transcription components.

The interplay between ubiquitination and phosphorylation has emerged as a prominent post-translational cross-talk and a key principle in regulating protein abundance, activity, and interactions. In some contexts, phosphorylation either generates phospho-degrons or induces conformational changes that are recognized by receptor proteins associated with the ubiquitin-proteasome degradation machinery (56). Consequently, phosphorylation can serve as an important regulatory switch that affects target protein ubiquitination and degradation. Because mTORC1 is an important kinase and regulator of MAF1, our studies also show mTORC1-dependent phosphorylation affects MAF1 protein ubiquitination and its turnover. Mutation of the major mTORC1 phosphorylation site, Ser-75, inhibits MAF1 ubiquitination and its turnover rate. These studies support the idea that the control of MAF1 stability is an important regulatory mode in response to cellular nutritional or other metabolic stress. However, it is worth noting that neither mTORC1 inhibition nor mutation of Ser-75 can completely block MAF1 turnover, suggesting the existence of other residues or motifs that are responsible for modulating its stability. Pradhan *et al.* (57) showed that the Tyr-166–Ser-167–Tyr-168 motif, particularly the Ser-167 residue, in the C-box was also critical for MAF1 stability. Moreover, human MAF1 is phosphorylated on multiple residues, many of which are highly conserved in vertebrates (19). Thus, further detailed studies will be required to determine whether other phosphorylation sites induced by other kinases are also involved in regulating MAF1 stability.

Our results identify an essential role for Cullin 2–based E3 ubiquitin ligases in MAF1 ubiquitination and turnover. Decreased CUL2 expression inhibited MAF1 degradation, suggesting that an intact E3 ligase-mediated ubiquitination system is both necessary and sufficient to sustain efficient MAF1 degradation by the proteasome. The CRLs constitute the major subfamily of E3 ligases that catalyze the transfer of ubiquitin from the E2-conjugating enzyme to the target substrate. Unlike other Cullin family members whose substrates have been frequently identified, only a few substrates of CUL2 have been revealed (58). CUL2 was originally predicted to function as a tumor suppressor because of its association with von Hippel–Lindau tumor-suppressor protein (VHL), which recognizes and mediates the degradation of some oncogenic protein substrates, such as HIFα (59), PKC (60), and epidermal growth factor receptor (61). However, pathogenic mutations in the CUL2 gene causing carcinoma has not been identified (62, 63), indicating that CUL2 may not function as a tumor suppressor protein. In support of this idea, CUL2 functions as a positive cell cycle regulator in *Caenorhabditis elegans* in a leucine-rich repeat protein-1 (LRR1)–dependent way (41). In human liver cancer, CUL2 can target tumor suppressor RhoB for degrada-

tion (64). Here, we also identified CUL2 as a major modulator of another tumor suppressor protein, MAF1. Although more studies are needed to identify which adaptor protein is responsible for recruiting MAF1 to the CUL2 complex, the present collective work suggests the idea that the function of CUL2 and its role in oncogenesis may dependent upon substrate recognition adaptor partners.

Recent studies suggested that dysregulation of tRNAs and tRNA derivatives play important roles in tumor development and progression. The regulation of both tRNAs and tRNA derivatives regulate the binding of Apaf-1 to cytochrome *c* to modulate the formation of the apoptosome and the subsequent activation of caspases (46, 47). Our present results support this notion, but it is likely that multiple mechanisms are involved in producing these changes. Vault RNAs (vtRNAs) are small (~100 nt long) polymerase III transcripts contained in the vault particles of eukaryotic cells (65). Expression of the vault RNA, particularly the vtRNA 1-1, protects cells from undergoing apoptosis (66, 67). In addition, both mature tRNAs and vtRNAs were reported to directly bind to chemotherapeutic compounds, like doxorubicin and mitoxantrone, to prevent the drug from reaching the site of action (68, 69).

Collectively, our studies provide novel links between CUL2-mediated regulation of MAF1, subsequent alterations in RNA pol III– dependent transcription, and the production of tRNAs to regulate apoptosis. Thus, loss of MAF1 in HCC and perhaps other cancer cells not only promotes oncogenesis but also mediates drug resistance by affecting the ability of these cells to undergo apoptosis.

Experimental procedures

Cell lines and reagents

All cell lines were cultured in Dulbecco's modified Eagle's medium supplemented with 10% fetal bovine serum, except MCF10A, which was cultured in Dulbecco's modified Eagle's medium/F-12 Ham's mixture supplemented with 5% equine serum, 20 ng/ml epidermal growth factor, 10 μg/ml insulin, 0.5 mg/ml hydrocortisone, 100 ng/ml cholera toxin, 100 units/ml penicillin, and 100 μg/ml streptomycin. The cells were incubated at 37 °C with 5% CO_2. MAF1-deficient ($MAF1^{-/-}$) murine embryonic fibroblasts (MEFs) were obtained from Dr. Nouria Hernandez lab from the University of Lausanne. HT29 cells engineered to express doxycycline-inducible MAF1–HA were generated as previously described (9). Plasmid DNAs and siRNAs (Table S1) were transfected with Lipofectamine 2000 and Lipofectamine RNAiMAX transfection reagent (Invitrogen), respectively, according to the manufacturer's protocols. The pcDNA3–MAF1–HA, pcDNA3–$MAF1^{S75A}$-HA, pcDNA3–$MAF1^{S75D}$–HA, and pcDNA–FLAG–FoxO1 expression vector was previously described (9, 21). The pCW7 construct, which contains cytomegalovirus-driven expression vectors for 6× His–Myc– ubiquitin, was obtained from Dr. D. M. Lonard (Department of Molecular and Cellular Biology, Baylor College of Medicine). The pcDNA3–$MAF1^{S60/68/75A}$–HA constructs were generated by mutating the indicated lysine to arginine using the QuikChange Lightning site-directed mutagenesis kit (Agilent Technologies) as the manufacturer's protocol with pcDNA3–MAF1–HA as the template. Primers for mutagenesis were designed using the Stratagene QuikChange primer design software. Mutagenesis was confirmed by sequencing at the Baylor College of Medicine/DNA Sequencing Core to ensure that only the intended mutation occurred.

Generation of $HepG2^{MAF1-HA}$ cells endogenously expressing HA-tagged MAF1 protein

The plasmid pSpCas9n(BB)-2A-GFP (PX461), Cas9n (D10A nickase mutant) from *Streptococcus pyogenes* with 2A-EGFP, and cloning backbone for sgRNA were gifts from the lab of Dr. Feng Zhang (Addgene plasmid no. 48140) (70). sgRNAs were designed using the online tool CRISPR Design developed by Zhang's laboratory and constructed as described previously (71). Target sequences of sgRNAs and PAGE-purified ultramer single-stranded donor oligonucleotides (ssODNs) used in this study are shown in Table S2. The CRISPR/Cas9 plasmids and single-stranded donor oligonucleotides (ssODNs) were cotransfected into HepG2 cells. Forty-eight hours after transfection, the cells were subjected to FACS sorting based on the expression of EGFP fluorescence. Single cells were plated in each well of 96-well plates. Confluent cell colonies were propagated and genotyped by Restriction Fragment Length Polymorphism (RFLP) assay and sequencing.

Reconstitution of $Maf1^{-/-}$ MEFs with ectopic expression of MAF1 S75A

Using the Gateway cloning method (Invitrogen), an amplicon corresponding to human *Maf1* cDNA containing the S75A mutation was amplified and cloned into the pDONR223 donor vector. Following sequencing to confirm the fidelity of the insert, MAF1–HA S75A was recloned into the pInducer20 lentiviral backbone vector. Lentivirus was produced in 293T cells by cotransfection of pInducer20 plasmids (with and without MAF1 inserts) with pMD2.G (vesicular stomatitis virus envelope protein (VSV-G) expression vector) and psPAX2 (packaging vector). Forty-eight hours after transfection, viral supernatants collected, sterile-filtered at 0.45 μm, and concentrated using the Lenti-X concentrator reagent (Takara). Concentrated virus was resuspended in PBS.

Immortalized $Maf1^{-/-}$ mouse embryonic fibroblasts were transduced with lentiviral particles for 24 h in the presence of Polybrene (8 μg/ml). After a 24-h recovery, transduced cells were selected by G418 for 7 days. pINDUCER-20 transgene expression was induced with 1 μg/ml doxycycline.

RNA isolation and quantitative real-time PCR

Total RNA was isolated from cells using the Zymo Directzol RNA kit. The RNAs were then reverse-transcribed into cDNA with the Superscript III first strand synthesis kit (Invitrogen). Real-time quantitative PCR was performed on the Lightcycler 480 (Roche) with a SYBR fast quantitative PCR kit (KAPA Biosystems). All reagents were validated by demonstrating a linear relationship between sample concentration and amplification kinetics over a three log range of nucleic acid concentrations, using cDNA made from total RNA from reference samples. Relative amounts of transcripts were quantified by comparative threshold cycle method ($\Delta\Delta Ct$) with GAPDH as the endoge-

nous reference control. The primers for targets are listed in Table S2. For graphical representation, $\Delta\Delta Ct$ values were normalized to controls and expressed as the difference of fold change.

Immunoblot analysis

The cells were washed with Dulbecco's Phosphate-Buffered Saline (DPBS) twice, then lysed in cell lysis buffer (20 mM Tris-Cl, pH 8.0, 150 mM sodium chloride, 1 mM EDTA, 1 mM EGTA, 2.5 mM sodium pyrophosphate, 1 mM β-glycerolphosphate, 1 mM sodium vanadate, 0.1% Triton X-100, supplemented with 0.1% protease inhibitor mixture set III (EMD Millipore)) for 20 min on ice, and sonicated for 5 s. After sonication, the cells were centrifuged for 20 min at 10,000 $\times$ *g*, and the supernatant was collected. The protein concentration was determined by using the Bio-Rad protein Dc assay. Cell lysates were equally subjected to immunoblot analysis and transferred onto a nitrocellulose membrane (GE Healthcare). After blocking with 5% nonfat milk in TBS with Tween 20, the membranes were incubated at 4 °C overnight with the primary antibodies. The antibodies used are listed in Table S3. After staining with horseradish peroxidase–linked secondary antibodies, signal detection was performed using a Clarity™ Western ECL substrate kit (Bio-Rad). Densitometric analysis was performed using ImageJ software (National Institutes of Health, Bethesda, MD).

Immunoprecipitation

For biochemical analyses of cytochrome *c* and Apaf1 protein interactions, the cells were rinsed twice with PBS and lysed in Nonidet P-40 lysis buffer (50 mM Tris-HCl, pH 8.0, 150 mM NaCl, 1% Nonidet P-40) supplemented with protease inhibitor mixture. The immunoprecipitation was carried out at 4 °C overnight by incubation of 1 μg of anti– cytochrome *c* antibody with cell extracts containing 2 mg of proteins, followed by addition of Dynabeads™ magnetic beads with recombinant protein G (Thermo Fisher Scientific) for another 2 h. Immunoprecipitates were collected and washed five times with lysis buffer, resuspended in SDS sample buffer, and boiled for 5 min at 95 °C. The bound proteins were detected for Apaf-1 protein by Western blotting.

Ubiquitination assay

Ubiquitination assays of ectopically expressed MAF1 were performed *in vivo* using either the Ni–NTA pulldown assays or immunoprecipitation of endogenous ubiquitin method. For Figs. 2*A*, 3*C*, and 4*C*, the cells were cotransfected with MAF1–HA and His– ubiquitin. Six hours before collecting, the cells were treated with 10 μM of MG132 where indicated. The cells were dissolved in lysis buffer (6 M guanidinium HCl, 0.1 M Na_2HPO_4/NaH_2PO_4, 0.01 M Tris-HCl, pH 8.0, 5 mM imidazole, and 10 mM β-mercaptoethanol). His-tagged proteins were captured using Ni^{2+}–NTA resin (Thermo Scientific) and eluted with imidazole. The presence of MAF1 protein in the eluted fraction was immunoblot analyzed using anti-HA antibody. For Fig. S2 (*C* and *D*), the cells were treated with 10 μM of MG132 for 6 h before collecting. The cells were washed with Dulbecco's Phosphate-Buffered Saline (DPBS) twice and then lysed in cell lysis buffer (50 mM Tris-HCl, pH 8.0, 150 mM NaCl, 1% Nonidet P-40) supplemented with protease inhibitor mixture. Noncovalent protein interactions were dissociated with 1% SDS and boiled for 10 min. Samples were diluted 10 times with cell lysis buffer. Lysates were incubated with Anti-HA magnetic beads (Pierce) at 4 °C for 4 h. The beads were washed three times with lysis buffer, and immunoprecipitates were separated from the beads by adding SDS loading sample buffer and were boiled and fractioned by SDS-PAGE. Immunoblot analysis was subsequently performed using the anti-ubiquitin or K48 linkage–specific polyubiquitin antibody.

Immunofluorescence

The cells, cultured in eight-chamber culture slides (Nunc), were rinsed with ice-cold PBS and fixed with 4% paraformaldehyde for 10 min at room temperature, followed by permeabilization with 0.2% Triton X-100 in PBS for 20 min and blocking in 2% BSA, 0.2% Triton X-100 in PBS for 60 min. For visualizing filamentous actin (F-actin), the cells were washed and directly stained with Phalloidin-iFluor 488 at room temperature for 1 h. For immunolocalizing MAF1–HA or p53, the cells were washed and subjected to immunofluorescence staining with the indicated primary antibodies at 4 °C overnight. The cells were then washed with cold PBS three times and incubated with Alexa 488 – or Alexa 594 – conjugated goat anti-rabbit or goat anti-rat IgGs (1:500, Molecular Probes) at room temperature for 1 h. After 4,6-diamidino-2-phenylindole (DAPI) staining, the slides were mounted in Fluoroshield histology mounting medium (Sigma–Aldrich) and sealed with nail polish, and the images were acquired using an Olympus (IX71) microscope equipped with DPController software (Olympus).

Cell cycle and apoptosis analysis

Cell cycle distribution was analyzed by flow cytometry. The cells were harvested, washed twice with PBS, and fixed in 70% ethanol overnight at −20 °C. Fixed cells were washed twice with PBS and incubated with 1 ml of PBS containing 10 μg/ml DAPI and 0.1% Triton X-100 for 30 min at 37 °C. Stained cells were analyzed using a BD Biosciences LSR II flow cytometer at the Baylor College of Medicine/Cytometry and Cell Sorting Core.

Induction of apoptosis caused by the cytotoxic effect of doxorubicin was evaluated by annexin V–FITC apoptosis detection kit (Sigma). The numbers of cells undergoing necrosis (positive for propidium iodide), early apoptosis (positive for Annexin V), and late apoptosis (double-positive for annexin V and propidium iodide) were quantified using flow cytometer as above.

MTS cell proliferation assay

Different siRNAs transfected HepG2 cells were incubated at 37 °C with 5% CO_2 for 48 h. Cell proliferation assay was performed using the MTS cell proliferation assay kit (Abcam) according to the manufacturer's instruction at 24 h after treatment with doxorubicin at the indicated concentrations. The experiments were repeated three times, and the data are represented as the means of quadruplicate wells ± S.E.

In vitro translation and proteasome degradation assay

Human MAF1–HA tagged protein were synthesized by using the TnT® quick-coupled transcription/translation sys-

tem (Promega) following the manufacturer's protocol with pcDNA3–MAF1–HA as the template. Degradation of *in vitro* translated MAF1 by was based on assays previously described (33). Briefly, *in vitro* translated protein was incubated with 20S proteasomes (1 μg; BioMol) in 20S assay buffer (20 mM Tris, pH 7.2, 1 mM EDTA, and 1 mM DTT) or with 26S proteasomes (1 μg; BioMol) in 26S assay buffer (20 mM Tris, pH 7.2, 25 mM KCl, 10 mM NaCl, 1 mM $MgCl_2$, 1 mM DTT, 4 mM ATP, 50 mM phosphocreatine, and 17.5 units/ml creatine phosphokinase), respectively, at 37 °C for 2 h. The reaction was stopped by addition of 6× SDS loading buffer. Samples were resolved by SDS-PAGE for immunoblotting.

Author contributions—X. W., J. J. L., and D. L. J. conceptualization; X. W., A. R., and C. J. W. data curation; X. W. and D. L. J. formal analysis; X. W. investigation; X. W., A. R., C. J. W., and J. J. L. methodology; X. W. writing-original draft; D. L. J. resources; D. L. J. funding acquisition; D. L. J. project administration; D. L. J. writing-review and editing.

Acknowledgment—We thank the cytometry and cell sorting core at Baylor College of Medicine for assistance with the cell cycle and apoptosis analysis.

References

1. Moir, R. D., and Willis, I. M. (2013) Regulation of pol III transcription by nutrient and stress signaling pathways. *Biochim. Biophys. Acta* **1829,** 361–375 CrossRef Medline
2. Boguta, M., Czerska, K., and Zoladek, T. (1997) Mutation in a new gene MAF1 affects tRNA suppressor efficiency in *Saccharomyces cerevisiae*. *Gene* **185,** 291–296 CrossRef Medline
3. Pluta, K., Lefebvre, O., Martin, N. C., Smagowicz, W. J., Stanford, D. R., Ellis, S. R., Hopper, A. K., Sentenac, A., and Boguta, M. (2001) MAF1p, a negative effector of RNA polymerase III in *Saccharomyces cerevisiae*. *Mol. Cell Biol.* **21,** 5031–5040 CrossRef Medline
4. Upadhya, R., Lee, J., and Willis, I. M. (2002) MAF1 is an essential mediator of diverse signals that repress RNA polymerase III transcription. *Mol. Cell* **10,** 1489–1494 CrossRef Medline
5. Abascal-Palacios, G., Ramsay, E. P., Beuron, F., Morris, E., and Vannini, A. (2018) Structural basis of RNA polymerase III transcription initiation. *Nature* **553,** 301–306 CrossRef Medline
6. Desai, N., Lee, J., Upadhya, R., Chu, Y., Moir, R. D., and Willis, I. M. (2005) Two steps in MAF1-dependent repression of transcription by RNA polymerase III. *J. Biol. Chem.* **280,** 6455–6462 CrossRef Medline
7. Vannini, A., Ringel, R., Kusser, A. G., Berninghausen, O., Kassavetis, G. A., and Cramer, P. (2010) Molecular basis of RNA polymerase III transcription repression by MAF1. *Cell* **143,** 59–70 CrossRef Medline
8. Johnson, S. S., Zhang, C., Fromm, J., Willis, I. M., and Johnson, D. L. (2007) Mammalian MAF1 is a negative regulator of transcription by all three nuclear RNA polymerases. *Mol. Cell* **26,** 367–379 CrossRef Medline
9. Palian, B. M., Rohira, A. D., Johnson, S. A., He, L., Zheng, N., Dubeau, L., Stiles, B. L., and Johnson, D. L. (2014) MAF1 is a novel target of PTEN and PI3K signaling that negatively regulates oncogenesis and lipid metabolism. *PLoS Genet.* **10,** e1004789 CrossRef Medline
10. Li, Y., Tsang, C. K., Wang, S., Li, X. X., Yang, Y., Fu, L., Huang, W., Li, M., Wang, H. Y., and Zheng, X. F. (2016) MAF1 suppresses AKT-mTOR signaling and liver cancer through activation of PTEN transcription. *Hepatology* **63,** 1928–1942 CrossRef Medline
11. Johnson, S. A., Dubeau, L., and Johnson, D. L. (2008) Enhanced RNA polymerase III–dependent transcription is required for oncogenic transformation. *J. Biol. Chem.* **283,** 19184–19191 CrossRef Medline
12. White, R. J. (2004) RNA polymerase III transcription and cancer. *Oncogene* **23,** 3208–3216 CrossRef Medline
13. Goodarzi, H., Liu, X., Nguyen, H. C., Zhang, S., Fish, L., and Tavazoie, S. F. (2015) Endogenous tRNA-derived fragments suppress breast cancer progression via YBX1 displacement. *Cell* **161,** 790–802 CrossRef Medline
14. Goodarzi, H., Nguyen, H. C. B., Zhang, S., Dill, B. D., Molina, H., and Tavazoie, S. F. (2016) Modulated expression of specific tRNAs drives gene expression and cancer progression. *Cell* **165,** 1416–1427 CrossRef Medline
15. Olvedy, M., Scaravilli, M., Hoogstrate, Y., Visakorpi, T., Jenster, G., and Martens-Uzunova, E. S. (2016) A comprehensive repertoire of tRNA-derived fragments in prostate cancer. *Oncotarget* **7,** 24766–24777 Medline
16. Pavon-Eternod, M., Gomes, S., Geslain, R., Dai, Q., Rosner, M. R., and Pan, T. (2009) tRNA over-expression in breast cancer and functional consequences. *Nucleic Acids Res.* **37,** 7268–7280 CrossRef Medline
17. Sun, C., Fu, Z., Wang, S., Li, J., Li, Y., Zhang, Y., Yang, F., Chu, J., Wu, H., Huang, X., Li, W., and Yin, Y. (2018) Roles of tRNA-derived fragments in human cancers. *Cancer Lett.* **414,** 16–25 CrossRef Medline
18. Kantidakis, T., Ramsbottom, B. A., Birch, J. L., Dowding, S. N., and White, R. J. (2010) mTOR associates with TFIIIC, is found at tRNA and 5S rRNA genes, and targets their repressor MAF1. *Proc. Natl. Acad. Sci. U.S.A.* **107,** 11823–11828 CrossRef Medline
19. Michels, A. A., Robitaille, A. M., Buczynski-Ruchonnet, D., Hodroj, W., Reina, J. H., Hall, M. N., and Hernandez, N. (2010) mTORC1 directly phosphorylates and regulates human MAF1. *Mol. Cell Biol.* **30,** 3749–3757 CrossRef Medline
20. Shor, B., Wu, J., Shakey, Q., Toral-Barza, L., Shi, C., Follettie, M., and Yu, K. (2010) Requirement of the mTOR kinase for the regulation of MAF1 phosphorylation and control of RNA polymerase III–dependent transcription in cancer cells. *J. Biol. Chem.* **285,** 15380–15392 CrossRef Medline
21. Rohira, A. D., Chen, C. Y., Allen, J. R., and Johnson, D. L. (2013) Covalent small ubiquitin-like modifier (SUMO) modification of MAF1 protein controls RNA polymerase III–dependent transcription repression. *J. Biol. Chem.* **288,** 19288–19295 CrossRef Medline
22. Tang, Z., Li, C., Kang, B., Gao, G., Li, C., and Zhang, Z. (2017) GEPIA: a web server for cancer and normal gene expression profiling and interactive analyses. *Nucleic Acids Res.* **45,** W98-W102 CrossRef Medline
23. Kudo, N., Matsumori, N., Taoka, H., Fujiwara, D., Schreiner, E. P., Wolff, B., Yoshida, M., and Horinouchi, S. (1999) Leptomycin B inactivates CRM1/exportin 1 by covalent modification at a cysteine residue in the central conserved region. *Proc. Natl. Acad. Sci. U.S.A.* **96,** 9112–9117 CrossRef Medline
24. Freedman, D. A., and Levine, A. J. (1998) Nuclear export is required for degradation of endogenous p53 by MDM2 and human papillomavirus E6. *Mol. Cell Biol.* **18,** 7288–7293 CrossRef Medline
25. Hochstrasser, M. (1996) Ubiquitin-dependent protein degradation. *Annu. Rev. Genet.* **30,** 405–439 CrossRef Medline
26. Akutsu, M., Dikic, I., and Bremm, A. (2016) Ubiquitin chain diversity at a glance. *J. Cell Sci.* **129,** 875–880 CrossRef Medline
27. Okumura, T., Ikeda, K., Ujihira, T., Okamoto, K., Horie-Inoue, K., Takeda, S., and Inoue, S. (2018) Proteasome 26S subunit PSMD1 regulates breast cancer cell growth through p53 protein degradation. *J. Biochem.* **163,** 19–29 CrossRef Medline
28. Dubiel, W., Pratt, G., Ferrell, K., and Rechsteiner, M. (1992) Purification of an 11 S regulator of the multicatalytic protease. *J. Biol. Chem.* **267,** 22369–22377 Medline
29. Chen, X., Barton, L. F., Chi, Y., Clurman, B. E., and Roberts, J. M. (2007) Ubiquitin-independent degradation of cell-cycle inhibitors by the REGγ proteasome. *Mol. Cell* **26,** 843–852 CrossRef Medline
30. Li, X., Amazit, L., Long, W., Lonard, D. M., Monaco, J. J., and O'Malley, B. W. (2007) Ubiquitin- and ATP-independent proteolytic turnover of p21 by the REGγ-proteasome pathway. *Mol. Cell* **26,** 831–842 CrossRef Medline
31. Li, X., Lonard, D. M., Jung, S. Y., Malovannaya, A., Feng, Q., Qin, J., Tsai, S. Y., Tsai, M. J., and O'Malley, B. W. (2006) The SRC-3/AIB1 coactivator is degraded in a ubiquitin- and ATP-independent manner by the REGγ proteasome. *Cell* **124,** 381–392 CrossRef Medline

32. Alvarez-Castelao, B., and Castaño, J. G. (2005) Mechanism of direct degradation of IκBα by 20S proteasome. *FEBS Lett.* **579,** 4797–4802 CrossRef Medline
33. Stewart, D. P., Koss, B., Bathina, M., Perciavalle, R. M., Bisanz, K., and Opferman, J. T. (2010) Ubiquitin-independent degradation of antiapoptotic MCL-1. *Mol. Cell Biol.* **30,** 3099–3110 CrossRef Medline
34. Wiggins, C. M., Tsvetkov, P., Johnson, M., Joyce, C. L., Lamb, C. A., Bryant, N. J., Komander, D., Shaul, Y., and Cook, S. J. (2011) BIM(EL), an intrinsically disordered protein, is degraded by 20S proteasomes in the absence of poly-ubiquitylation. *J. Cell Sci.* **124,** 969–977 CrossRef Medline
35. Zhao, Y., Li, X., Cai, M. Y., Ma, K., Yang, J., Zhou, J., Fu, W., Wei, F. Z., Wang, L., Xie, D., and Zhu, W. G. (2013) XBP-1u suppresses autophagy by promoting the degradation of FoxO1 in cancer cells. *Cell Res.* **23,** 491–507 CrossRef Medline
36. Hunter, T. (2007) The age of crosstalk: phosphorylation, ubiquitination, and beyond. *Mol. Cell* **28,** 730–738 CrossRef Medline
37. Petroski, M. D., and Deshaies, R. J. (2005) Function and regulation of cullin–RING ubiquitin ligases. *Nat. Rev. Mol. Cell Biol.* **6,** 9–20 CrossRef Medline
38. Soucy, T. A., Smith, P. G., Milhollen, M. A., Berger, A. J., Gavin, J. M., Adhikari, S., Brownell, J. E., Burke, K. E., Cardin, D. P., Critchley, S., Cullis, C. A., Doucette, A., Garnsey, J. J., Gaulin, J. L., Gershman, R. E., *et al.* (2009) An inhibitor of NEDD8-activating enzyme as a new approach to treat cancer. *Nature* **458,** 732–736 CrossRef Medline
39. Tanimoto, K., Makino, Y., Pereira, T., and Poellinger, L. (2000) Mechanism of regulation of the hypoxia-inducible factor-1α by the von Hippel–Lindau tumor suppressor protein. *EMBO J.* **19,** 4298–4309 CrossRef Medline
40. Ernens, I., Goodfellow, S. J., Innes, F., Kenneth, N. S., Derblay, L. E., White, R. J., and Scott, P. H. (2006) Hypoxic stress suppresses RNA polymerase III recruitment and tRNA gene transcription in cardiomyocytes. *Nucleic Acids Res.* **34,** 286–294 CrossRef Medline
41. Starostina, N. G., Simpliciano, J. M., McGuirk, M. A., and Kipreos, E. T. (2010) CRL2(LRR-1) targets a CDK inhibitor for cell cycle control in *C. elegans* and actin-based motility regulation in human cells. *Dev. Cell* **19,** 753–764 CrossRef Medline
42. Yamaguchi, H., and Condeelis, J. (2007) Regulation of the actin cytoskeleton in cancer cell migration and invasion. *Biochim. Biophys. Acta* **1773,** 642–652 CrossRef Medline
43. Le Grazie, M., Biagini, M. R., Tarocchi, M., Polvani, S., and Galli, A. (2017) Chemotherapy for hepatocellular carcinoma: the present and the future. *World J. Hepatol.* **9,** 907–920 CrossRef Medline
44. Wu, L., Pan, J., Thoroddsen, V., Wysong, D. R., Blackman, R. K., Bulawa, C. E., Gould, A. E., Ocain, T. D., Dick, L. R., Errada, P., Dorr, P. K., Parkinson, T., Wood, T., Kornitzer, D., Weissman, Z., *et al.* (2003) Novel small-molecule inhibitors of RNA polymerase III. *Eukaryot. Cell* **2,** 256–264 CrossRef Medline
45. Teichmann, M., Dieci, G., Pascali, C., and Boldina, G. (2010) General transcription factors and subunits of RNA polymerase III: paralogs for promoter- and cell type-specific transcription in multicellular eukaryotes. *Transcription* **1,** 130–135 CrossRef Medline
46. Mei, Y., Yong, J., Liu, H., Shi, Y., Meinkoth, J., Dreyfuss, G., and Yang, X. (2010) tRNA binds to cytochrome c and inhibits caspase activation. *Mol. Cell* **37,** 668–678 CrossRef Medline
47. Saikia, M., Jobava, R., Parisien, M., Putnam, A., Krokowski, D., Gao, X. H., Guan, B. J., Yuan, Y., Jankowsky, E., Feng, Z., Hu, G. F., Pusztai-Carey, M., Gorla, M., Sepuri, N. B., Pan, T., *et al.* (2014) Angiogenin-cleaved tRNA halves interact with cytochrome c, protecting cells from apoptosis during osmotic stress. *Mol. Cell Biol.* **34,** 2450–2463 CrossRef Medline
48. Bross, P. F., Kane, R., Farrell, A. T., Abraham, S., Benson, K., Brower, M. E., Bradley, S., Gobburu, J. V., Goheer, A., Lee, S. L., Leighton, J., Liang, C. Y., Lostritto, R. T., McGuinn, W. D., Morse, D. E., *et al.* (2004) Approval summary for bortezomib for injection in the treatment of multiple myeloma. *Clin. Cancer Res.* **10,** 3954–3964 CrossRef Medline
49. Fennell, D. A., Chacko, A., and Mutti, L. (2008) BCL-2 family regulation by the 20S proteasome inhibitor bortezomib. *Oncogene* **27,** 1189–1197 CrossRef Medline
50. Lee, K. B., Wang, D., Lippard, S. J., and Sharp, P. A. (2002) Transcription-coupled and DNA damage-dependent ubiquitination of RNA polymerase II *in vitro*. *Proc. Natl. Acad. Sci. U.S.A.* **99,** 4239–4244 CrossRef Medline
51. Li, H., Zhang, Z., Wang, B., Zhang, J., Zhao, Y., and Jin, Y. (2007) Wwp2-mediated ubiquitination of the RNA polymerase II large subunit in mouse embryonic pluripotent stem cells. *Mol. Cell Biol.* **27,** 5296–5305 CrossRef Medline
52. Mitsui, A., and Sharp, P. A. (1999) Ubiquitination of RNA polymerase II large subunit signaled by phosphorylation of carboxyl-terminal domain. *Proc. Natl. Acad. Sci. U.S.A.* **96,** 6054–6059 CrossRef Medline
53. Wang, Z., Wu, C., Aslanian, A., Yates, J. R., 3rd, and Hunter, T. (2018) Defective RNA polymerase III is negatively regulated by the SUMO-Ubiquitin-Cdc48 pathway. *Elife* **7,**
54. Leśniewska, E., Cieśla, M., and Boguta, M. (2019) Repression of yeast RNA polymerase III by stress leads to ubiquitylation and proteasomal degradation of its largest subunit, C160. *Biochim. Biophys. Acta Gene Regul. Mech.* **1862,** 25–34 CrossRef Medline
55. Wang, F., Zhao, K., Yu, S., Xu, A., Han, W., and Mei, Y. (2019) RNF12 catalyzes BRF1 ubiquitination and regulates RNA polymerase III–dependent transcription. *J. Biol. Chem.* **294,** 130–141 CrossRef Medline
56. Holt, L. J. (2012) Regulatory modules: Coupling protein stability to phosphoregulation during cell division. *FEBS Lett.* **586,** 2773–2777 CrossRef Medline
57. Pradhan, A., Hammerquist, A. M., Khanna, A., and Curran, S. P. (2017) The C-box region of MAF1 regulates transcriptional activity and protein stability. *J. Mol. Biol.* **429,** 192–207 CrossRef Medline
58. Wang, S., Xia, W., Qiu, M., Wang, X., Jiang, F., Yin, R., and Xu, L. (2016) Atlas on substrate recognition subunits of CRL2 E3 ligases. *Oncotarget* **7,** 46707–46716 Medline
59. Maxwell, P. H., Wiesener, M. S., Chang, G. W., Clifford, S. C., Vaux, E. C., Cockman, M. E., Wykoff, C. C., Pugh, C. W., Maher, E. R., and Ratcliffe, P. J. (1999) The tumour suppressor protein VHL targets hypoxia-inducible factors for oxygen-dependent proteolysis. *Nature* **399,** 271–275 CrossRef Medline
60. Okuda, H., Saitoh, K., Hirai, S., Iwai, K., Takaki, Y., Baba, M., Minato, N., Ohno, S., and Shuin, T. (2001) The von Hippel–Lindau tumor suppressor protein mediates ubiquitination of activated atypical protein kinase C. *J. Biol. Chem.* **276,** 43611–43617 CrossRef Medline
61. Zhou, L., and Yang, H. (2011) The von Hippel–Lindau tumor suppressor protein promotes c-Cbl–independent poly-ubiquitylation and degradation of the activated EGFR. *PLoS One* **6,** e23936 CrossRef Medline
62. Clifford, S. C., Astuti, D., Hooper, L., Maxwell, P. H., Ratcliffe, P. J., and Maher, E. R. (2001) The pVHL-associated SCF ubiquitin ligase complex: molecular genetic analysis of elongin B and C, Rbx1 and HIF-1α in renal cell carcinoma. *Oncogene* **20,** 5067–5074 CrossRef Medline
63. Duerr, E. M., Gimm, O., Neuberg, D. S., Kum, J. B., Clifford, S. C., Toledo, S. P., Maher, E. R., Dahia, P. L., and Eng, C. (1999) Differences in allelic distribution of two polymorphisms in the VHL-associated gene CUL2 in pheochromocytoma patients without somatic CUL2 mutations. *J. Clin. Endocrinol. Metab.* **84,** 3207–3211 CrossRef Medline
64. Xu, J., Li, L., Yu, G., Ying, W., Gao, Q., Zhang, W., Li, X., Ding, C., Jiang, Y., Wei, D., Duan, S., Lei, Q., Li, P., Shi, T., Qian, X., Qin, J., and Jia, L. (2015) The neddylation–cullin 2–RBX1 E3 ligase axis targets tumor suppressor RhoB for degradation in liver cancer. *Mol. Cell Proteomics* **14,** 499–509 CrossRef Medline
65. Stadler, P. F., Chen, J. J., Hackermüller, J., Hoffmann, S., Horn, F., Khaitovich, P., Kretzschmar, A. K., Mosig, A., Prohaska, S. J., Qi, X., Schutt, K., and Ullmann, K. (2009) Evolution of vault RNAs. *Mol. Biol. Evol.* **26,** 1975–1991 CrossRef Medline
66. Amort, M., Nachbauer, B., Tuzlak, S., Kieser, A., Schepers, A., Villunger, A., and Polacek, N. (2015) Expression of the vault RNA protects cells from undergoing apoptosis. *Nat. Commun.* **6,** 7030 CrossRef Medline
67. Chen, J., OuYang, H., An, X., and Liu, S. (2018) Vault RNAs partially induces drug resistance of human tumor cells MCF-7 by binding to the RNA/DNA-binding protein PSF and inducing oncogene GAGE6. *PLoS One* **13,** e0191325 CrossRef Medline

68. Agudelo, D., Bourassa, P., Beauregard, M., Bérubé, G., and Tajmir-Riahi, H. A. (2013) tRNA binding to antitumor drug doxorubicin and its analogue. *PLoS One* **8,** e69248 CrossRef Medline
69. Gopinath, S. C., Matsugami, A., Katahira, M., and Kumar, P. K. (2005) Human vault-associated non-coding RNAs bind to mitoxantrone, a chemotherapeutic compound. *Nucleic Acids Res.* **33,** 4874–4881 CrossRef Medline
70. Ding, Q., Regan, S. N., Xia, Y., Oostrom, L. A., Cowan, C. A., and Musunuru, K. (2013) Enhanced efficiency of human pluripotent stem cell genome editing through replacing TALENs with CRISPRs. *Cell Stem Cell* **12,** 393–394 CrossRef Medline
71. Mali, P., Yang, L., Esvelt, K. M., Aach, J., Guell, M., DiCarlo, J. E., Norville, J. E., and Church, G. M. (2013) RNA-guided human genome engineering via Cas9. *Science* **339,** 823–826 CrossRef Medline